



## Research article

# LncRNA Zfas1 boosts cell apoptosis and autophagy in myocardial injury induced by hypoxia via miR-383-5p/ATG10 axis

Miaomiao Liu, Ying Zhang, Yongxin Li, Tao Shi, Yang Yan\*

Cardiovascular Surgery, The First Affiliated Hospital of Xi'an Jiaotong University, Shaanxi, China

## ARTICLE INFO

## Keywords:

Zfas1  
miR-383-5p  
ATG10  
Myocardial injury

## ABSTRACT

**Background:** Myocardial injury has been regarded as a major cause of several heart diseases. Long non-coding RNA (lncRNA) has emerged as a key regulator in a wide array of diseases.

**Aim of the study:** This study aims to explore the role of Zfas1 in myocardial injury.

**Methods:** 3-(4,5-dimethylthiazol-2-yl)-2,5-diphenyltetrazolium bromide (MTT) assay was adopted to evaluate the proliferative capability of H9c2 cells. Terminal deoxynucleotidyltransferase dUTP nick end labeling (TUNEL) and flow cytometry assays were employed to measure cell apoptosis. The expression of proteins related to apoptosis and autophagy was examined by Western blot. Immunofluorescence (IF) assay was performed to monitor the process of autophagy. Real-time reverse-transcription polymerase chain reaction (RT-qPCR) was employed to determine the expressions of autophagy-related gene 10 (ATG10), miR-383-5p and Zfas1. The interacting relationship between miR-383-5p and ATG10 (or Zfas1) was assessed by luciferase reporter and RNA-binding protein immunoprecipitation (RIP) assays.

**Results:** The treatment of hypoxia hindered cell proliferation but accelerated cell apoptosis and autophagy. ATG10 exhibited higher mRNA and protein expression in H9c2 cells induced by hypoxia. MiR-383-5p was revealed to be the upstream gene of ATG10 and could interact with ATG10. Zfas1 was validated to sponge miR-383-5p and positively regulated ATG10 expression. Zfas1 knockdown-mediated cellular proliferation, apoptosis and autophagy phenotypes were counteracted by ATG10 abundance.

**Conclusions:** LncRNA Zfas1 boosts cell apoptosis and autophagy in myocardial injury induced by hypoxia via miR-383-5p/ATG10 axis, indicating that Zfas1 may be utilized as a therapeutic target for myocardial injury.

## 1. Introduction

Myocardial injury has been uncovered to be a major cause of heart diseases, including myocardial infarction, myocarditis and coronary heart disease, which lead to increasing mortalities all over the world [1–3]. Worse still, the pathology of myocardial injury is complicated [4], and sensitive diagnostic and therapeutic methods at molecular level for patients afflicted with myocardial injury remains unclear [5]. Therefore, better understanding of major pathologic mechanisms contributing to myocardial injury is urgently required.

Characterized by cytoplasmic vacuolization, autophagy is a process of lysosome-dependent degradation [6]. Aside from serving as

\* Corresponding author. 277 West Yanta Road, Xi'an 710007, Shaanxi, China.

E-mail address: [maggielmm@163.com](mailto:maggielmm@163.com) (M. Liu).

<https://doi.org/10.1016/j.heliyon.2024.e24578>

Received 14 February 2023; Received in revised form 29 December 2023; Accepted 10 January 2024

Available online 18 January 2024

2405-8440/© 2024 Published by Elsevier Ltd.

This is an open access article under the CC BY-NC-ND license

(<http://creativecommons.org/licenses/by-nc-nd/4.0/>).

a degradative pathway, autophagy is closely associated with many diseases and tumors, such as endometriosis and doxorubicin resistance in malignancies [7,8]. Autophagy has been increasingly reported to be an essential therapeutic target in a panel of diseases, including cardiovascular diseases. Of note, autophagy-related genes (ATGs) have been elucidated to be closely associated with autophagy in impacting several cellular processes of multiple diseases, even cancers [9–11]. Recently, autophagy-related gene 10 (ATG10) was reported to modulate the formation of autophagosome in lung cancer [12]. Additionally, ATG10 protects the osteogenic ability of periodontal ligament stem cells in rats [13]. Nevertheless, the role of ATG10 in myocardial injury remains unclear.

Accumulating evidence has verified that long non-coding RNAs (lncRNAs) could be involved in the competitive endogenous RNA (ceRNA) network by sponging shared microRNA (miRNA) with messenger RNA (mRNA) to offset the repressive effect of miRNA on mRNA expression [14,15]. It has been found that a large number of lncRNAs sponge certain miRNAs and function as ceRNAs in modulating gene expression, thus exerting profound impacts on the initiation and development of multiple diseases. For example, lncRNA MIAT promotes cardiac hypertrophy via sequestering miR-93 to up-regulate TLR4 expression [16]. lncRNA-H19 as a ceRNA can hinder Akt activation to hamper angiogenesis, thereby contributing to the treatment of diabetic wounds [17]. Previous studies have revealed that Zfas1 positively regulates ST6GAL1 expression by interacting with miR-150, thus modulating sialylation of EGFR in T-cell acute lymphoblastic leukemia [18]. In addition, Zfas1 sequesters miR-10a to overexpress SKA1, thereby facilitating proliferation and migration of clear cell renal cell carcinoma [19]. However, whether Zfas1 can affect disease-related gene via ceRNA regulatory mechanism in myocardial injury remains to be investigated.

In our research, we discovered that lncRNA Zfas1 accelerates cell apoptosis and autophagy in myocardial injury induced by hypoxia via miR-383-5p/ATG10 axis, which implied a novel therapeutic tactic for patients confronted with myocardial injury.

## 2. Materials and methods

### 2.1. Cell culture and treatment

H9c2 cells were available from the American type culture collection (ATCC; Manassas, VA) for our study and maintained in Dulbecco's modified eagle medium (DMEM; Invitrogen, Carlsbad, CA), with 10 % fetal bovine serum (FBS; Invitrogen), 1 % GlutaMAX and 1 % Penicillin/Streptomycin (100 U/ml:100 mg/ml; Invitrogen) as medium supplements. Cell culture was implemented in a humid atmosphere at 37 °C containing 5 % CO<sub>2</sub>. To induce myocardial injury via hypoxia, H9c2 cells were incubated in an incubator at 37 °C with only 3 % O<sub>2</sub>. Cells under normoxia condition (21 % O<sub>2</sub>) served as control.

### 2.2. Real-time reverse-transcription polymerase chain reaction (RT-qPCR)

According to manufacturer's guidelines, TRIzol reagent (Invitrogen) was utilized to extract total RNA from cultured H9c2 cells. For lncRNA and mRNA analysis, a Reverse Transcription Kit (Takara, Shiga, Japan) was adopted to synthesize the first-strand cDNA. For miRNA analysis, a microRNA First-Strand cDNA Synthesis Kit (Sangon Biotech, Shanghai, China) was applied in the process of reverse transcription. The amplification reaction was operated with SYBR-Green PCR Master Mix kit (Applied Biosystems, Foster City, CA) or TaqMan miRNA assay kit (Applied Biosystems) on a 7900HT Fast Real-Time System (Applied Biosystems). The relative gene expression was computed using the  $2^{-\Delta\Delta Ct}$  method with GAPDH or U6 as the endogenous control. Bio-repeats were conducted in triplicate.

### 2.3. Transfection plasmids

The short hairpin RNAs (shRNAs) targeting ATG10 (sh-ATG10#1/2) with negative control (sh-NC) or Zfas1 (sh-Zfas1#1/2) with negative control (sh-NC) and miR-383-5p mimics with negative control (NC mimics) were synthesized by GenePharma (Shanghai, China). For ATG10 overexpression, the overexpression vector was constructed by ligating sequence of ATG10 into pcDNA3.1 (GenePharma). The above-mentioned vectors were transfected into H9c2 cells through using Lipofectamine 2000 (Invitrogen) according to the manufacturer's instruction. Experiment was conducted in triplicate.

### 2.4. 3-(4,5-Dimethylthiazol-2-yl)-2,5-diphenyltetrazolium bromide (MTT) assay

After transfection, H9c2 cells ( $5 \times 10^3$  cells/well) were inoculated in 96-well plates and incubated for 48 h. Then 20  $\mu$ L of 5 mg/ml MTT solution (Sigma-Aldrich, St. Louis, MO) was added to each well. After 4 h of incubation, 150  $\mu$ L of dimethyl sulfoxide (DMSO; Sigma-Aldrich) was added to each well and mixed for 10 min. The OD value was read at 490 nm. Bio-repeats were conducted in triplicate.

### 2.5. Terminal deoxynucleotidyltransferase dUTP nick end labeling (TUNEL) assay

According to the protocol of TUNEL assay, H9c2 cell apoptosis was detected in line with In Situ Cell Death Detection kit (Roche, Basel, Switzerland). Cell nuclei were detected using 4',6-diamidino-2-phenylindole (DAPI) staining. Apoptosis was evaluated by counting the TUNEL-positive cells as well as the DAPI-positive cells at five random fields under fluorescence microscope using Image-Pro Plus 6.0 software. Bio-repeats were conducted in triplicate.

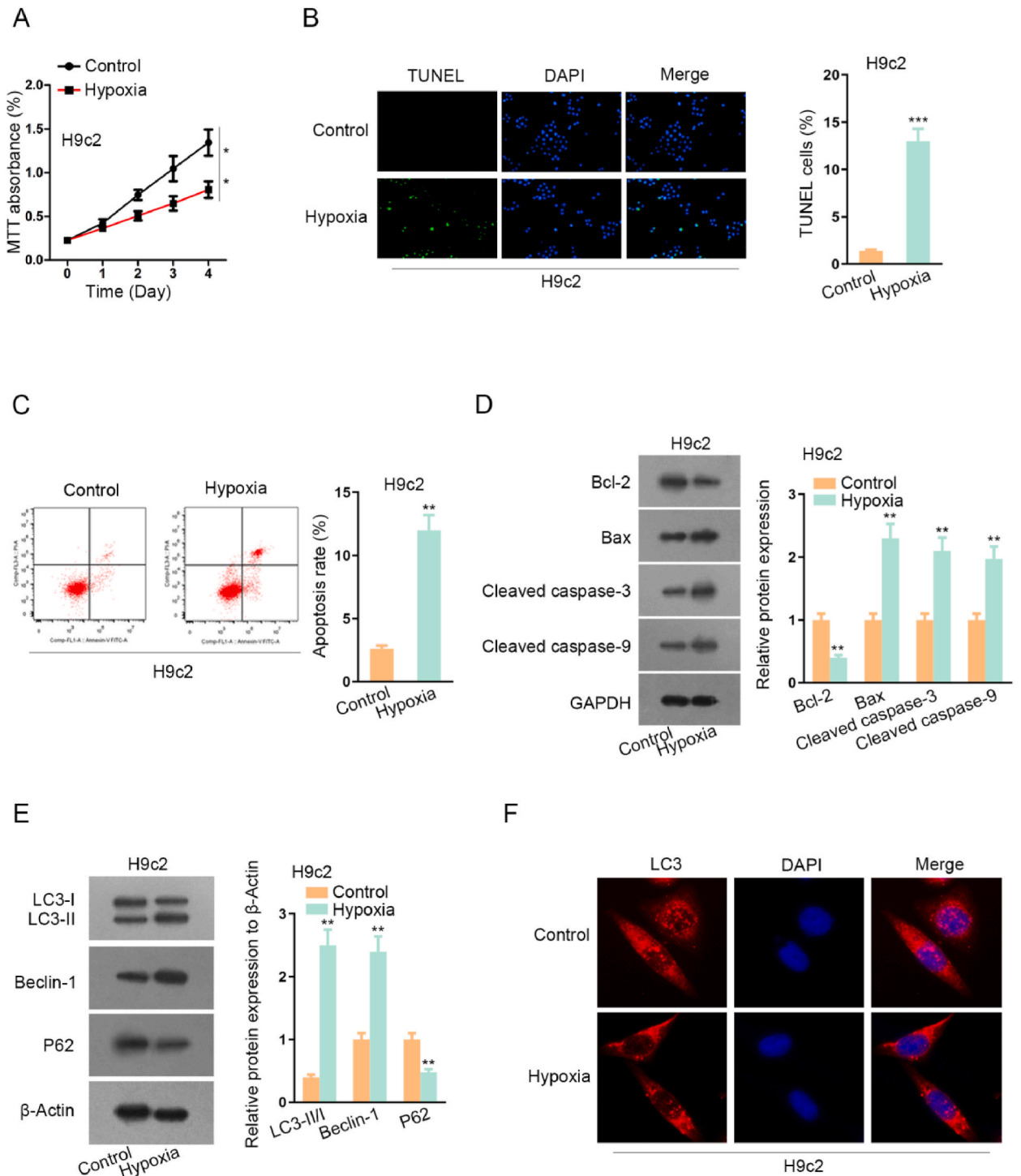


**Fig. 1.** Myocardial injury was induced by hypoxia in H9c2 cells. (A) MTT assay was conducted to evaluate cell proliferation. (B–C) TUNEL and flow cytometry assays were finalized to measure cell apoptosis. (D–E) Western blot assay was adopted to examine the levels of proteins associated with apoptosis (Bcl-2, Bax, cleaved caspase-3, and cleaved caspase-9) and autophagy (LC3-I, LC3-II, Beclin-1 and P62). (F) IF assay was performed to detect LC3 protein expression. \*\* $P < 0.01$ , \*\*\* $P < 0.001$ .

## 2.6. Flow cytometry assay

H9c2 cells ( $1 \times 10^4$  cells/well) were incubated in 6-well plates with DMEM in different atmosphere. H9c2 cells were cultured for 24 h at 37 °C in a 5 % CO<sub>2</sub> incubator with 3 % or 21 % O<sub>2</sub> concentration. Then, H9c2 cells were collected and immobilized in 75 % ethanol at 4 °C overnight. On the following day, after purified with PBS, H9c2 cells were double stained using Annexin V-FITC/PI detection kit (Invitrogen) in the dark for 30 min at room temperature. Finally, stained H9c2 cells were analyzed using flow cytometry. Bio-repeats were conducted in triplicate.

## 2.7. Western blot

Cells were dissolved by radio immunoprecipitation assay (RIPA) buffer supplied with protease and phosphatase inhibitors (Roche). Cell proteins were separated by 10 % sodium dodecyl sulfate-polyacrylamide gel electrophoresis. After electrophoresis, proteins were transferred onto polyvinylidene difluoride (PVDF) membrane. The membrane was obstructed in 5 % skimmed milk and mixed with primary antibodies overnight at 4 °C. After purifying and incubation, the membranes were incubated with secondary antibodies (1:2000) at room temperature. Protein bands were detected by the ECL chemiluminescent Detection System (Thermo Fisher Scientific, Rochester, NY). Bio-repeats were conducted in triplicate.

## 2.8. Immunofluorescence assay (IF)

H9c2 cells were fixed with 4 % paraformaldehyde for 30 min, and then permeabilized with 0.5 % Triton X-100 solution. The goat serum was adopted to obstruct cells. Additionally, H9c2 cells were cultivated with proper primary antibodies at 4 °C overnight, and then incubated with adjacent secondary antibodies at 37 °C for 1 h. Finally, H9c2 cells were stained by DAPI, and observed by fluorescent microscope. Bio-repeats were conducted in triplicate.

## 2.9. Luciferase reporter assay

The 3' untranslated region (3' UTR) sequences of ATG10 containing miR-383-5p wild-type binding site or mutant variant were subcloned into the pmirGLO vector (Promega, Madison, WI) to produce ATG10-WT and ATG10-Mut vectors. Then, wild-type Zfas1 reporter (Zfas1-WT) and the mutant-type Zfas1 reporter (Zfas1-Mut) were also constructed. The constructs were co-transfected into H9c2 cells with miR-383-5p mimics or NC mimics by the use of Lipofectamine 2000. After 48 h of incubation, luciferase activities were measured by Dual-Luciferase Reporter Assay System (Promega). Bio-repeats were conducted in triplicate.

## 2.10. RNA-binding protein immunoprecipitation (RIP) assay

RIP assay was carried out through Magna RNA-binding protein immunoprecipitation kit (Millipore, Billerica, MA). Briefly, cell lysate (H9c2 cells) was incubated in RIP buffer containing magnetic beads conjugating Argonaute 2 (Ago2) antibody (Millipore). Immunoglobulin G (IgG) antibody (Millipore) acted as control. Immunoprecipitated RNA was isolated, purified, and then analyzed by RT-qPCR analysis. Bio-repeats were conducted in triplicate.

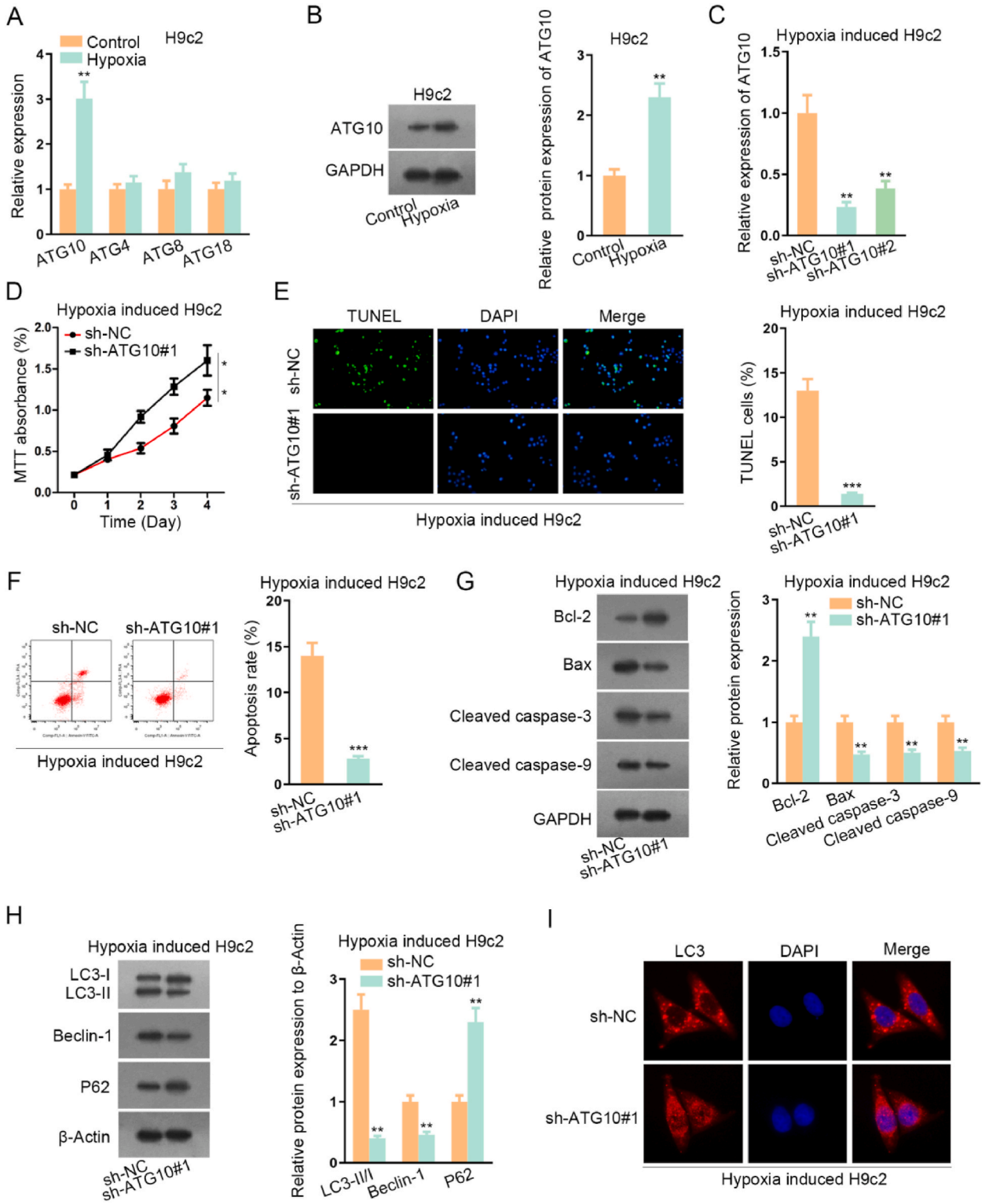
## 2.11. Statistical analysis

All experiments were operated at least three times ( $N \geq 3$ ), and results were presented as the mean  $\pm$  standard deviation. To analyze statistical difference, the p-values between groups were calculated by student's t-test or one-way/two-way analysis of variance (ANOVA) using Graphpad 6.0 statistical software (GraphPad Software Inc., San Diego, CA), with significant result collected when  $p < 0.05$ .

# 3. Result

## 3.1. Myocardial injury was induced by hypoxia treatment in H9c2 cells

Hypoxia has been frequently reported to induce myocardial injury [20]. Hence, H9c2 cells were subjected to hypoxia treatment to mimic myocardial injury. To evaluate the cellular phenotype of H9c2 cells after hypoxia treatment, functional experiments were finalized. MTT assay suggested that the vitality of H9c2 cells was impaired by hypoxia induction (Fig. 1A). On the contrary, TUNEL assay revealed a prominent increase in the TUNEL-positive cells by hypoxia treatment compared with control (without hypoxia treatment) group (Fig. 1B). Moreover, the fraction of apoptotic cells was augmented dramatically in hypoxia-treated H9c2 cells (Fig. 1C). In contrast with control group, hypoxia treatment resulted in an evident decrease of Bcl-2 protein expression, while a notable increase in the protein levels of Bax, cleaved caspase-3 and cleaved caspase-9 (Fig. 1D). To examine whether the autophagic flux is activated in H9c2 cells, the protein level of autophagy-associated proteins, including LC3-I, LC3-II, Beclin-1 and P62 was assessed by Western blot in the different groups. P62 served as a typical marker of autophagic flux, and the accumulation of P62 expression implied disrupted autophagic flux. Western blot results indicated that the ratio of LC3-II/I, and Beclin-1 protein expression were prominently up-regulated, while P62 protein level was down-regulated in response to hypoxia treatment in H9c2 cells compared with the control



(caption on next page)

### Fig. 2. ATG10 inhibition alleviated injury of myocardial injury hypoxia-treated H9c2 cells.

(A) The expression of ATG10, ATG4, ATG8 and ATG18 was tested by RT-qPCR. (B) The protein expression of ATG10 was determined by Western blot. (C) The knockdown efficiency of ATG10 in hypoxia-treated H9c2 cells was explored by RT-qPCR. (D) Cell proliferation was studied by MTT assay after knockdown of ATG10. (E–F) Cell apoptosis was assessed by TUNEL and flow cytometry assays after knockdown of ATG10. (G–H) Western blot assay was employed to monitor expression levels of proteins related with apoptosis and autophagy after knockdown of ATG10. (I) IF assay was carried out to detect LC3 protein expression. \*\*P < 0.01, \*\*\*P < 0.001.

group (Fig. 1E). IF assay also revealed that hypoxia treatment caused an aggregation of autophagy marker protein LC3 (Fig. 1F). Taken together, myocardial injury was successfully induced by hypoxia treatment in H9c2 cells through hampering cell proliferation and stimulating cell apoptosis and autophagy.

### 3.2. ATG10 inhibition alleviated myocardial injury in hypoxia-treated H9c2 cells

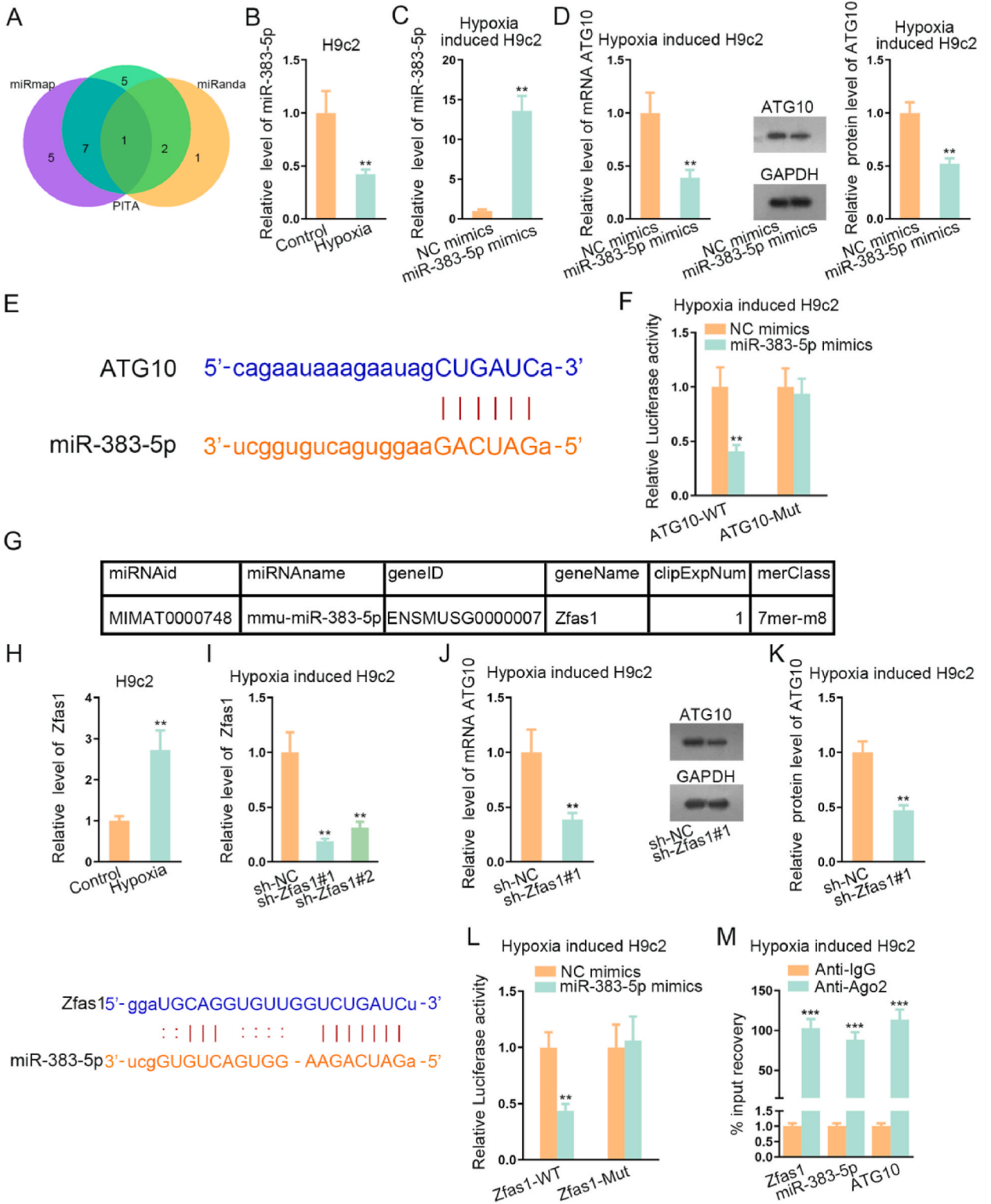
Multiple researches have unveiled that ATGs act as important roles in several cellular processes, especially cell autophagy in many diseases or cancers [21]. We hypothesized that ATG might play a part in myocardial injury. Therefore, we explored whether the expression of several key ATGs, including ATG4, ATG8, ATG10 and ATG18 is induced by hypoxia treatment in H9c2 cells. The results showed that only ATG10 expression was conspicuously up-regulated by hypoxia induction, while other ATGs (ATG4, ATG8, ATG18) indicated no evident alternation between control and hypoxia groups (Fig. 2A). Similarly, the protein expression of ATG10 was also up-regulated in H9c2 cells in hypoxia treatment (Fig. 2B). Prior to loss-of-function assays, we forced the down-regulation of ATG10 by transfecting specific shRNAs. ATG10 mRNA expression was markedly decreased by transfecting sh-ATG10#1 or sh-ATG10#2 into hypoxia-induced H9c2 cells. We noticed that sh-ATG10#1 exhibited a better knockdown efficiency than sh-ATG10#2 (Fig. 2C). Thus, sh-ATG10#1 was chose for the following loss-of-function assay. To begin with, MTT assay suggested that the cell vitality was greatly enhanced by ATG10 knockdown in hypoxia-treated H9c2 cells (Fig. 2D). Then, the transfection of sh-ATG10#1 into hypoxia-treated H9c2 cells triggered an obvious attenuation of cell apoptosis through TUNEL assay (Fig. 2E). Likewise, flow cytometry assay demonstrated that the apoptosis rate plummeted by sh-ATG10#1 transfection in hypoxia-treated H9c2 cells (Fig. 2F). Furthermore, the protein level of Bcl-2 was elevated, but those of Bax, cleaved caspase-3 and cleaved caspase-9 were decreased by ATG10 down-regulation in hypoxia-treated H9c2 cells (Fig. 2G). To verify whether ATG10 participated in the modulation of autophagy, we performed Western blot assay. Western blot data uncovered that ATG10 deficiency evidently reduced the ratio of LC3-II/I and the protein level of Beclin-1, but elevated P62 protein expression, indicating the suppression on autophagy flux (Fig. 2H). IF assay also validated that autophagy was inhibited by ATG10 suppression, as LC3 was down-regulated (Fig. 2I). To conclude, ATG10 inhibition alleviated myocardial injury hypoxia-treated H9c2 cells.

### 3.3. LncRNA Zfas1 acted as a ceRNA to regulate ATG10 expression by sponging miR-383-5p

Growing evidence has proved that mRNA could be modulated by lncRNA in the ceRNA network, where lncRNA release mRNA from miRNA induced silencing complex via competitively interacting with miRNA. Thus, we speculated there might exist upstream layer of molecular regulation for the biological functions of ATG10. StarBase was adopted to predict the potential miRNAs that may bind to ATG10. MiR-383-5p was screened out according the prediction of three websites, those are miRmap, PITA and miRanda (Fig. 3A). Then, we discovered miR-383-5p expression was down-regulated in hypoxia-treated H9c2 cells (Fig. 3B). MiR-383-5p expression was greatly up-regulated by miR-383-5p mimics transfection into hypoxia-treated H9c2 cells (Fig. 3C). Furthermore, the mRNA and protein levels of ATG10 were down-regulated by miR-383-5p mimics transfection (Fig. 3D). The binding site of miR-383-5p on the sequence of ATG10 was predicted by starBase (Fig. 3E). Luciferase reporter assay showed that miR-383-5p overexpression caused an obvious reduction of ATG10-WT vector luciferase activity, while no alteration was observed in ATG10-Mut vector (Fig. 3F). We then searched potential lncRNAs that may bind with miR-383-5p. Zfas1 was screened out with the screening criterion set as medium stringency ( $\geq 2$ ) of CLIP data (Fig. 3G). Subsequent RT-qPCR assay showcased that Zfas1 expression was up-regulated in H9c2 cells treated by hypoxia (Fig. 3H). According to RT-qPCR assay, Zfas1 expression was reduced by transfecting sh-Zfas1#1 or sh-Zfas1#2 into hypoxia-treated H9c2 cells. Particularly, sh-Zfas1#1 achieved a better knockdown outcome than sh-Zfas1#2 (Fig. 3I). Interestingly, the mRNA and protein expression of ATG10 declined distinctly in response to Zfas1 repression, indicating the plausible ceRNA role of Zfas1 (Fig. 3J). As shown in Fig. 3K, the potential binding site of miR-383-5p on Zfas1 was predicted. Luciferase reporter assay performed in hypoxia-treated H9c2 cells manifested that the luciferase activity of pmirGLO-Zfas1-WT was hampered by miR-383-5p abundance, but that of pmirGLO-Zfas1-Mut displayed no meaningful difference (Fig. 3L). Finally, ATG10, miR-383-5p and Zfas1 were discovered to be enriched by Ago2 antibody rather than IgG antibody, implying that these three genes could be immunoprecipitated by anti-Ago2 instead of anti-IgG (Fig. 3M). Collectively, lncRNA Zfas1 acted as a ceRNA to regulate ATG10 expression by sponging miR-383-5p.

### 3.4. LncRNA Zfas1 promoted cell apoptosis and autophagy in myocardial injury through ATG10

To verify whether Zfas1 promoted cell apoptosis and autophagy in hypoxia-induced H9c2 cells by regulating ATG10, rescue assays were conducted. We found that the depletion of ATG10 mRNA and protein expression caused by Zfas1 suppression was abrogated by ATG10 abundance (Fig. 4A). Next, MTT assay indicated that the promoting effect of Zfas1 inhibition on cell proliferation was reversed



(caption on next page)

**Fig. 3.** LncRNA Zfas1 acted as a ceRNA to regulate ATG10 expression by sponging miR-383-5p.

(A) The possible upstream miRNAs that may interact with ATG10 were predicted and screened out. (B–C) The expression of miR-383-5p and the overexpression efficiency of miR-383-5p mimics was investigated by RT-qPCR. (D) The effect of miR-383-5p overexpression on ATG10 expression at mRNA and protein levels were studied by RT-qPCR and Western blot respectively. (E) The binding sites of miR-383-5p on the 3' UTR sequences of ATG10 were shown. (F) Luciferase reporter assay validated the binding relationship between miR-383-5p and ATG10. (G) Zfas1 was screened out as the probable gene that may bind with miR-383-5p through bioinformatics tool. (H–I) The expression and knockdown efficiency of Zfas1 was investigated by RT-qPCR. (J) The regulation of Zfas1 on ATG10 was explored by RT-qPCR and Western blot. (K) The putative binding sites of miR-383-5p on Zfas1. (L) Luciferase reporter assay proved the physical interaction between miR-383-5p and Zfas1. (M) RIP assay showcased that ATG10, miR-383-5p and Zfas1 were co-immunoprecipitated by antibody targeting Ago2. \*\*P < 0.01, \*\*\*P < 0.001.

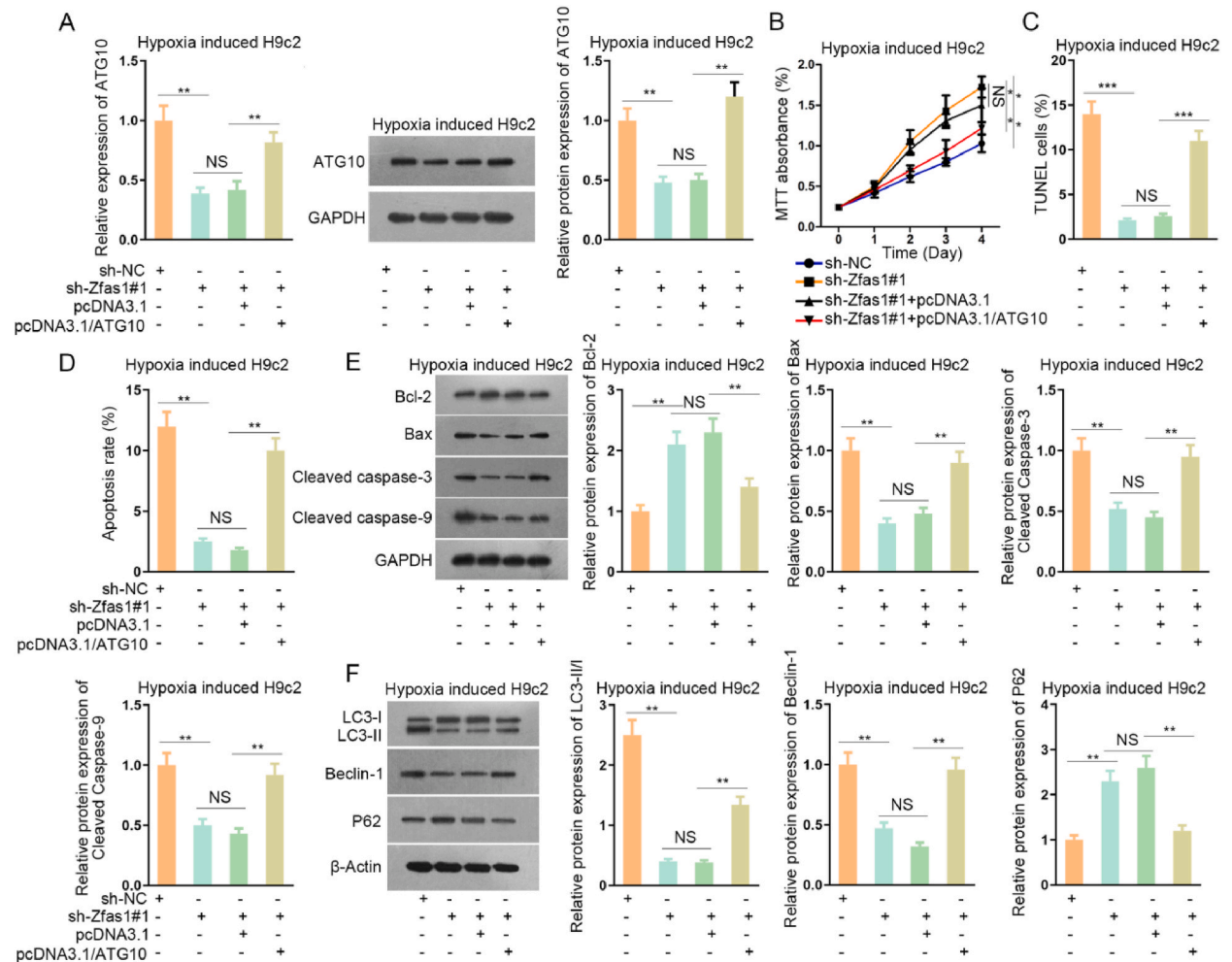


**Fig. 4.** LncRNA Zfas1 promoted cell apoptosis and autophagy in myocardial injury through ATG10.

(A) The mRNA and protein levels of ATG10 were respectively measured by RT-qPCR and Western blot. (B) Cell proliferation was evaluated by MTT assay in a rescue manner. (C–D) Cell apoptosis was examined by TUNEL and flow cytometry assays in a rescue manner. (E–F) Western blot assay was performed to detect the expression of protein associated with apoptosis and autophagy in a rescue manner. \*\*P < 0.01, \*\*\*P < 0.001. NS stands for not significant.

by ATG10 overexpression (Fig. 4B). TUNEL assay illustrated that ATG10 overexpression counteracted the inhibitory impact of Zfas1 knockdown on cell apoptosis (Fig. 4C). Flow cytometry further validated this conclusion, which indicated that the inhibitory effect of Zfas1 knockdown on the apoptosis rate was abolished by co-transfecting pcDNA3.1/ATG10 (Fig. 4D). Besides, sh-Zfas1-mediated increase of Bcl-3, yet decrease of Bax, cleaved caspase-3 and cleaved caspase-9 protein levels were reversed by co-transfecting pcDNA3.1/ATG10 into hypoxia-induced H9c2 cells (Fig. 4E). Lastly, ATG10 overexpression counteracted Zfas1-knockdown elicited decrease on LC3-II/I ratio and Beclin-1 protein level, as well as the elevation on P62 protein level (Fig. 4F). The above data convincingly demonstrated that lncRNA Zfas1 promoted cell apoptosis and autophagy in myocardial injury induced by hypoxia through ATG10.

#### 4. Discussion

Contributing to the development of multiple heart diseases, myocardial injury has gained increasing attention from researches [22]. In spite of great advances made in the diagnosis and treatment for some cardiovascular diseases, such as acute myocardial infarct, the deep pathology behind myocardial injury remains poorly understood [23]. In our study, myocardial injury model was constructed by hypoxia treatment in H9c2 cells. Functional experiments manifested that hypoxia induction hampered cell proliferation but boosted cell apoptosis and autophagy.

Autophagy is a ubiquitous phenomenon in eukaryotes where lysosomes remove long-lived proteins and organelles that are damaged, denatured or senescent [24,25]. Additionally, autophagy was reported to play a protective role in hypoxia injury [26]. Autophagy can be activated in a variety of ways, but the specific mechanism remains elusive. ATG10, as a member of ATGs, has been identified to be involved in diverse cellular process, including autophagy [12,27,28]. For instance, ATG10 gene was closely associated with VKH syndrome in Chinese Han population [29]. ATG10 also participated in lymphovascular invasion and lymph node migration of colorectal cancer cells [30]. In our study, we discovered that ACT10 presented significantly higher expression in H9c2 cells treated with hypoxia, and ATG10 inhibition promoted cell proliferation, while refrained cell apoptosis and autophagy.

Accumulating investigations that mRNA could be silenced by miRNAs, which specifically binding to 3' UTR of target gene [31]. Intriguingly, lncRNAs can serve as a ceRNA to bind with miRNAs through miRNA response elements (MREs), which adds another layer of regulation on the target gene of miRNAs [32]. Notably, ceRNA network was proved to be closely related to several biological processes [33]. Based on this theory, we hypothesized that ATG10 may function as a target gene in a ceRNA network. Herein, miR-383-5p was predicted and screened out to specifically bind with the 3' UTR region of ATG10. The former studies have disclosed the roles of miR-383-5p in ceRNA networks. For instance, circCRIM1 modulates ZEB2 axis through acting as a sponge for miR-383-5p [34]; RP11-284F21.9 competitively binds to miR-383-5p to up-regulate MAL2 expression [35]. In this study, we found that both the mRNA and protein levels of ATG10 were negatively regulated by miR-383-5p, adding strong evidence to the mutual binding relationship between miR-383-5p and ATG10. Additionally, Zfas1 was predicted and confirmed to bind with miR-383-5p. It was reported that Zfas1 can target downstream miRNA to modulate cardiac dysfunction [36]. RIP assay in our study showed the co-existence of Zfas1, miR-383-5p and ATG10 in RNA-induced silencing complex. We then implemented rescue assays and identified that ATG10 abundance rescued the ameliorating effects on cell proliferation, apoptosis and autophagy elicited by Zfas1 deficiency in hypoxia-treated H9c2 cells. The above results confirmed that Zfas1 acts as a ceRNA by targeting miR-383-5p/ATG10 axis.

Collectively, our exploration initially investigated the Zfas1/miR-383-5p/ATG10 regulatory axis in myocardial injury induced by hypoxia. Mechanically, we discovered that lncRNA Zfas1 boosts cell apoptosis and autophagy in myocardial injury induced by hypoxia via sponging miR-383-5p to positively regulate ATG10. However, our study just made a preliminary research on the possible regulatory mechanism of Zfas1 in myocardial injury, other potential regulatory mechanisms still needs to be further explored. In the future study, we will take into consideration the roles of transcription factors and RNA-binding proteins, in order to provide in-depth investigation of Zfas1.

#### Data availability statement

The data used to support the findings of this study are included within the article.

#### CRediT authorship contribution statement

**Miaomiao Liu:** Data curation, Formal analysis, Investigation, Methodology, Resources, Software, Supervision, Validation, Visualization, Writing – original draft, Writing – review & editing. **Ying Zhang:** Data curation, Formal analysis, Investigation, Resources, Visualization, Writing – original draft, Writing – review & editing. **Yongxin Li:** Data curation, Formal analysis, Software, Supervision, Writing – original draft, Writing – review & editing. **Tao Shi:** Data curation, Formal analysis, Resources, Software, Validation, Writing – original draft, Writing – review & editing. **Yang Yan:** Conceptualization, Formal analysis, Project administration, Validation, Writing – original draft, Writing – review & editing.

#### Declaration of competing interest

The authors declare that they have no conflict of interest.

#### References

- [1] W.K. Kim, C. Liebetrau, A. van Linden, J. Blumenstein, L. Gaede, C.W. Hamm, T. Walther, H. Mollmann, Myocardial injury associated with transcatheter aortic valve implantation (TAVI), *Clin. Res. Cardiol.: Off. J. German Cardiac Societ.* 105 (5) (2016) 379–387.
- [2] L. Lu, M. Liu, R. Sun, Y. Zheng, P. Zhang, Myocardial infarction: symptoms and treatments, *Cell Biochem. Biophys.* 72 (3) (2015) 865–867.
- [3] M. Madjid, O. Fatemi, Components of the complete blood count as risk predictors for coronary heart disease: in-depth review and update, *Tex. Heart Inst. J.* 40 (1) (2013) 17–29.
- [4] D. Matsiukevich, G. Piraino, P. Lahni, P.W. Hake, V. Wolfe, M. O'Connor, J. James, B. Zingarelli, Metformin ameliorates gender-and age-dependent hemodynamic instability and myocardial injury in murine hemorrhagic shock, *Biochim. Biophys. Acta, Mol. Basis Dis.* 1863 (10 Pt B) (2017) 2680–2691.
- [5] X. Chen, H. Guo, Q. Li, Y. Zhang, H. Liu, X. Zhang, K. Xie, Z. Zhu, Q. Miao, S. Su, Protective effect of berberine on aconite-induced myocardial injury and the associated mechanisms, *Mol. Med. Rep.* 18 (5) (2018) 4468–4476.
- [6] R. Nagar, Autophagy: a brief overview in perspective of dermatology, *Indian J. Dermatol. Venereol. Leprol.* 83 (3) (2017) 290–297.

- [7] C. Chen, L. Lu, S. Yan, H. Yi, H. Yao, D. Wu, G. He, X. Tao, X. Deng, Autophagy and doxorubicin resistance in cancer, *Anti Cancer Drugs* 29 (1) (2018) 1–9.
- [8] L. Zhan, J. Li, B. Wei, Autophagy in endometriosis: friend or foe? *Biochem. Biophys. Res. Commun.* 495 (1) (2018) 60–63.
- [9] M. Mauthe, F. Reggiori, ATG proteins: are we always looking at autophagy? *Autophagy* 12 (12) (2016) 2502–2503.
- [10] W. Huang, X. Zhao, Y. Tian, T. Cao, Y. Li, Z. Liu, Y. Jing, S. Wang, C. Gao, L. Yu, Outcomes of peripheral blood stem cell transplantation patients from HLA-mismatched unrelated donor with antithymocyte globulin (ATG)-Thymoglobulin versus ATG-Fresenius: a single-center study, *Med. Oncol.* 32 (2) (2015) 465.
- [11] I. Koyama-Honda, K. Tsuboyama, N. Mizushima, ATG conjugation-dependent degradation of the inner autophagosomal membrane is a key step for autophagosome maturation, *Autophagy* 13 (7) (2017) 1252–1253.
- [12] K. Xie, C. Liang, Q. Li, C. Yan, C. Wang, Y. Gu, M. Zhu, F. Du, H. Wang, J. Dai, X. Liu, G. Jin, H. Shen, H. Ma, Z. Hu, Role of ATG10 expression quantitative trait loci in non-small cell lung cancer survival, *Int. J. Cancer* 139 (7) (2016) 1564–1573.
- [13] K. Zhang, F. Liu, D. Jin, T. Guo, R. Hou, J. Zhang, B. Lu, Y. Hou, X. Zhao, Y. Li, Autophagy preserves the osteogenic ability of periodontal ligament stem cells under high glucose conditions in rats, *Arch. Oral Biol.* 101 (2019) 172–179.
- [14] Y. Zhan, Y. Li, B. Guan, Z. Wang, D. Peng, Z. Chen, A. He, S. He, Y. Gong, X. Li, L. Zhou, Long non-coding RNA HNF1A-AS1 promotes proliferation and suppresses apoptosis of bladder cancer cells through upregulating Bcl-2, *Oncotarget* 8 (44) (2017) 76656–76665.
- [15] X. Wang, K.B. Hu, Y.Q. Zhang, C.J. Yang, H.H. Yao, Comprehensive analysis of aberrantly expressed profiles of lncRNAs, miRNAs and mRNAs with associated ceRNA network in cholangiocarcinoma, *Cancer Biomarkers: Section A Disease markers* 23 (4) (2018) 549–559.
- [16] Y. Li, J. Wang, L. Sun, S. Zhu, LncRNA myocardial infarction-associated transcript (MIAT) contributed to cardiac hypertrophy by regulating TLR4 via miR-93, *Eur. J. Pharmacol.* 818 (2018) 508–517.
- [17] S.C. Tao, B.Y. Rui, Q.Y. Wang, D. Zhou, Y. Zhang, S.C. Guo, Extracellular vesicle-mimetic nanovesicles transport LncRNA-H19 as competing endogenous RNA for the treatment of diabetic wounds, *Drug Deliv.* 25 (1) (2018) 241–255.
- [18] Q. Liu, H. Ma, X. Sun, B. Liu, Y. Xiao, S. Pan, H. Zhou, W. Dong, L. Jia, The regulatory ZFAS1/miR-150/ST6GAL1 crosstalk modulates sialylation of EGFR via PI3K/Akt pathway in T-cell acute lymphoblastic leukemia, *J. Exp. Clin. Cancer Res.* : CR 38 (1) (2019) 199.
- [19] D. Dong, Z. Mu, N. Wei, M. Sun, W. Wang, N. Xin, Y. Shao, C. Zhao, Long non-coding RNA ZFAS1 promotes proliferation and metastasis of clear cell renal cell carcinoma via targeting miR-10a/SKA1 pathway, *Biomed. Pharmacotherap* = *Biomed. Pharmacotherapie* 111 (2019) 917–925.
- [20] X. Guo, X. Gu, S. Harehwaree, X. Rong, L. Li, M. Chu, Induced pluripotent stem cell-conditional medium inhibits H9C2 cardiomyocytes apoptosis via autophagy flux and Wnt/beta-catenin pathway, *J. Cell Mol. Med.* 23 (6) (2019) 4358–4374.
- [21] I. Vergne, F. Lafont, L. Espert, A. Esclatine, M. Biard-Piechaczyk, [Autophagy, ATG proteins and infectious diseases], *M-S (Med. Sci.) : M/S.* 33 (3) (2017) 312–318.
- [22] S.J. Clark, M. Eisenhut, D. Sidaras, S.W. Hancock, P. Newland, K. Thorburn, Myocardial injury in infants ventilated on the paediatric intensive care unit: a case control study, *Crit. Care* 10 (5) (2006) R128.
- [23] M. Takaoka, S. Uemura, H. Kawata, K. Imagawa, Y. Takeda, K. Nakatani, N. Naya, M. Horii, S. Yamano, Y. Miyamoto, Y. Yoshimasa, Y. Saito, Inflammatory response to acute myocardial infarction augments neointimal hyperplasia after vascular injury in a remote artery, *Arterioscler. Thromb. Vasc. Biol.* 26 (9) (2006) 2083–2089.
- [24] J. Mialet-Perez, C. Vindis, Autophagy in health and disease: focus on the cardiovascular system, *Essays Biochem.* 61 (6) (2017) 721–732.
- [25] T. Nam, J.H. Han, S. Devkota, H.W. Lee, Emerging paradigm of crosstalk between autophagy and the ubiquitin-proteasome system, *Mol. Cell.* 40 (12) (2017) 897–905.
- [26] G. Guan, L. Yang, W. Huang, J. Zhang, P. Zhang, H. Yu, S. Liu, X. Gu, Mechanism of interactions between endoplasmic reticulum stress and autophagy in hypoxia/reoxygenation-induced injury of H9c2 cardiomyocytes, *Mol. Med. Rep.* 20 (1) (2019) 350–358.
- [27] Y.K. Jo, S.A. Roh, H. Lee, N.Y. Park, E.S. Choi, J.H. Oh, S.J. Park, J.H. Shin, Y.A. Suh, E.K. Lee, D.H. Cho, J.C. Kim, Polypyrimidine tract-binding protein 1-mediated down-regulation of ATG10 facilitates metastasis of colorectal cancer cells, *Cancer Lett.* 385 (2017) 21–27.
- [28] A. Catanese, F. Olde Heuvel, M. Mulaw, M. Demestre, J. Higelin, G. Barbi, A. Freischmidt, J.H. Weishaupt, A.C. Ludolph, F. Roselli, T.M. Boeckers, Retinoic acid worsens ATG10-dependent autophagy impairment in TBK1-mutant hiPSC-derived motoneurons through SQSTM1/p62 accumulation, *Autophagy* (2019) 1–19.
- [29] M. Zheng, H. Yu, L. Zhang, H. Li, Y. Liu, A. Kijlstra, P. Yang, Association of ATG5 gene polymorphisms with behcet's disease and ATG10 gene polymorphisms with VKH syndrome in a Chinese han population, *Invest. Ophthalmol. Vis. Sci.* 56 (13) (2015) 8280–8287.
- [30] Y.K. Jo, S.C. Kim, I.J. Park, S.J. Park, D.H. Jin, S.W. Hong, D.H. Cho, J.C. Kim, Increased expression of ATG10 in colorectal cancer is associated with lymphovascular invasion and lymph node metastasis, *PLoS One* 7 (12) (2012) e52705.
- [31] J.K. Li, C. Chen, J.Y. Liu, J.Z. Shi, S.P. Liu, B. Liu, D.S. Wu, Z.Y. Fang, Y. Bao, M.M. Jiang, J.H. Yuan, L. Qu, L.H. Wang, Long noncoding RNA MRCAT1 promotes metastasis of clear cell renal cell carcinoma via inhibiting NPR3 and activating p38-MAPK signaling, *Mol. Cancer* 16 (1) (2017) 111.
- [32] C. Song, J. Zhang, H. Qi, C. Feng, Y. Chen, Y. Cao, L. Ba, B. Ai, Q. Wang, W. Huang, C. Li, H. Sun, The global view of mRNA-related ceRNA cross-talks across cardiovascular diseases, *Sci. Rep.* 7 (1) (2017) 10185.
- [33] F. Conte, G. Ficon, M. Chiara, T. Colombo, L. Farina, P. Paci, Role of the long non-coding RNA PVT1 in the dysregulation of the ceRNA-ceRNA network in human breast cancer, *PLoS One* 12 (2) (2017) e0171661.
- [34] Y. Du, X. Liu, S. Zhang, S. Chen, X. Guan, Q. Li, X. Chen, Y. Zhao, CircCRIM1 promotes ovarian cancer progression by working as ceRNAs of CRIM1 and targeting miR-383-5p/ZEB2 axis, *Reprod. Biol. Endocrinol.* : RB&E 19 (1) (2021) 176.
- [35] B. Shao, X. Fu, X. Li, Y. Li, N. Gan, RP11-284F21.9 promotes oral squamous cell carcinoma development via the miR-383-5p/MAL2 axis, *J. Oral Pathol. Med.* 49 (1) (2020) 21–29, official publication of the International Association of Oral Pathologists and the American Academy of Oral Pathology.
- [36] J.J. Liu, Y. Li, M.S. Yang, R. Chen, C.Q. Cen, SP1-induced ZFAS1 aggravates sepsis-induced cardiac dysfunction via miR-590-3p/NLRP3-mediated autophagy and pyroptosis, *Arch. Biochem. Biophys.* 695 (2020) 108611.